

Multiscale structure of calcium- and magnesium-silicate-hydrate gels

Wei-Shan Chiang¹, Giovanni Ferraro², Emiliano Fratini², Francesca Ridi², Yi-Qi Yeh³, U-Ser Jeng³, Sow-Hsin Chen^{1,*} and Piero Baglioni^{2,*}

¹Department of Nuclear Science and Engineering, Massachusetts Institute of Technology, Cambridge, MA, USA.

²Department of Chemistry “Ugo Schiff” and CSGI, University of Florence, via della Lastruccia 3-Sesto Fiorentino, I-50019, Florence, Italy.

³National Synchrotron Radiation Research Center, Hsinchu Science Park, Hsinchu 30076, Taiwan.

*Corresping authors email: piero.baglioni@unifi.it, sowhsin@mit.edu

Electronic Supplementary Information

The complete list of all the gels investigated in this work is reported in Table S0.

Table S0. Chemical composition of the different silicate hydrates investigated.

Sample Label	Target composition	Chemical Route
MSH	Mg/Si=1	double-decomposition ^a
MSH*	Mg/Si=1	solid oxides ^b
CSH-A	Ca/Si=1	double-decomposition ^c
CSH-B	Ca/Si=1.4	double-decomposition ^c
CSH-C	Ca/Si=1, Culminal	double-decomposition ^c
Mixed	Ca/Mg=1, (Ca+Mg)/Si=1	double-decomposition ^{a,c}

^a Na₂SiO₃·4H₂O (≥99% Sigma-Aldrich), Mg(NO₃)₂·6H₂O (98-102%KT, Sigma-Aldrich).

^b MgO (≥99% Sigma-Aldrich, average size: 44 μm), Silica Fumed (≥99% Sigma-Aldrich, average size: 0.007 μm).

^c Na₂SiO₃·4H₂O (≥99% Sigma-Aldrich), Ca(NO₃)₂·4H₂O (≥99% Sigma-Aldrich).

Analytical form of the small-angle X-ray scattering (SAXS) model: $\langle \overline{P(Q)} \rangle$

Here we describe below the expression of $\langle \overline{P(Q)} \rangle$ for the two different cases (C-S-H and M-S-

H). $\langle \overline{P(Q)} \rangle$ is the normalized intra-particle structure factor averaged over the distribution of the

size and all possible orientations of the globules. We also describe a combined model for the mixed case in the end.

C-S-H case

Based on the previous studies of some of the authors,^{1,2} the structure of the C-S-H globule can be modeled as a disk with layered sub-structure. The size distribution of the C-S-H globules is assumed to come from the “effective” Schultz distribution of the number of repeating layers n of the multi-layered disk. Therefore, $\langle \overline{P(Q)} \rangle$ equals to $\langle \overline{P(Q)} \rangle_{Orientation,n}$ and it can be mathematically expressed by equation (S1).

$$\langle \overline{P(Q)} \rangle_{Orientation,n} = \int_0^{\infty} \langle \overline{P(Q,n)} \rangle_{Orientation} f_S(n) dn, \quad (S1)$$

where

$$\langle \overline{P(Q,n)} \rangle_{Orientation} = \int_0^1 \overline{P(Q,\mu,n)} d\mu, \quad (S2)$$

$$f_S(n) = \left(\frac{Z_n + 1}{\bar{n}} \right)^{Z_n + 1} n^{Z_n} \exp \left[- \left(\frac{Z_n + 1}{\bar{n}} \right) n \right] / \Gamma(Z_n + 1) \quad Z_n > -1, \quad (S3)$$

$$\overline{P(Q,\mu,n)} = \left| \overline{F(Q,\mu,n)} \right|^2 = \left[\frac{2J_1 \left(QR\sqrt{1-\mu^2} \right)}{QR\sqrt{1-\mu^2}} \right]^2 C^2 (A^2 + B^2), \quad (S4)$$

$$A = \chi \cos \left(\frac{Q\mu(nL - L_2)}{2} \right) \frac{\sin \left(\frac{Q\mu L_1}{2} \right)}{Q\mu} + \cos \left(\frac{Q\mu(nL + L_1)}{2} \right) \frac{\sin \left(\frac{Q\mu L_2}{2} \right)}{Q\mu}, \quad (S5)$$

$$B = \chi \sin\left(\frac{Q\mu(nL - L_2)}{2}\right) \frac{\sin\left(\frac{Q\mu L_1}{2}\right)}{Q\mu} + \sin\left(\frac{Q\mu(nL + L_1)}{2}\right) \frac{\sin\left(\frac{Q\mu L_2}{2}\right)}{Q\mu}, \quad (\text{S6})$$

$$C = \frac{2}{n[\chi L_1 + L_2]} \frac{\sin\left(\frac{Q\mu nL}{2}\right)}{\sin\left(\frac{Q\mu L}{2}\right)}, \quad (\text{S7})$$

$$\text{and } \chi = \frac{\rho_1 - \rho_s}{\rho_2 - \rho_s}. \quad (\text{S8})$$

The fitting parameters of the intra-particle structure factor of the C-S-H samples are the disk radius, R , the layer thickness of hydration water, L_1 , and the layer thickness of hydrated calcium silicate, L_2 , the scattering length density contrast ratio $\chi = \frac{\rho_1 - \rho_s}{\rho_2 - \rho_s}$ (ρ_1 , ρ_2 , and ρ_s are scattering length densities (SLDs) of hydrated water, hydrated calcium silicate, and solvent, respectively), the average number of repeating layers inside a globule, \bar{n} , the width parameter Z_n of the number of layers described by a Schultz distribution. The equivalent radius R_e in $S(Q)$ can be calculated as $R_e = (3\bar{n}R^2L/4)^{(1/3)}$, where $L = L_1 + L_2$ is the interlayer distance, and the total thickness t can be found by $t = nL$.

M-S-H case

In the M-S-H cases (see Fig. S1) the high- Q peak characteristic of the layered sub-structure, which is the essential feature of the C-S-H samples, is not present. In addition, there is a broad bump in the high- Q part of the SAXS pattern. These observations allow us to use a simple model of polydisperse spheres to describe the intra-particle structure factor. We denote the normalized intra-particle structure factor averaged over the radius of the polydisperse spheres as

$$\langle \overline{P(Q)} \rangle_R = \int_0^{\infty} \overline{P(Q, R)}_{sphere} f_S(R) dR, \quad (\text{S9})$$

$$\text{where } \overline{P(Q, R)}_{sphere} = \left\{ \frac{3[\sin(QR) - (QR)\cos(QR)]}{(QR)^3} \right\}^2. \quad (\text{S10})$$

We assume the distribution of the sphere radius to be Schultz distribution and therefore

$$f_S(R) = \left(\frac{Z_R + 1}{\bar{R}} \right)^{Z_R + 1} R^{Z_R} \exp\left[-\left(\frac{Z_R + 1}{\bar{R}} \right) R \right] / \Gamma(Z_R + 1). \quad (\text{S11})$$

The essential fitting parameters of the intra-particle structure factor of the M-S-H samples are the average radius \bar{R} of the spheres and the width parameter Z_R of the Schultz distribution of the sphere radius. The equivalent radius R_e in $S(Q)$ is equal to \bar{R} .

Mixed case

Based on the description above, we analyze the mixed sample through a combined model, assuming that the interaction between C-S-H and M-S-H components is negligible at the length-

scale studied by SAXS ($\sim 1\text{-}2000 \text{ \AA}$). Consequently, we can express the scattering intensity of SAXS by adding together the intensity contribution from both C-S-H and M-S-H components:

$$I(Q) = N_{CSH} \langle \overline{P(Q)} \rangle_{CSH} S(Q)_{c,CSH} + N_{MSH} \langle \overline{P(Q)} \rangle_{MSH} S(Q)_{c,MSH} + bkg . \quad (\text{S12})$$

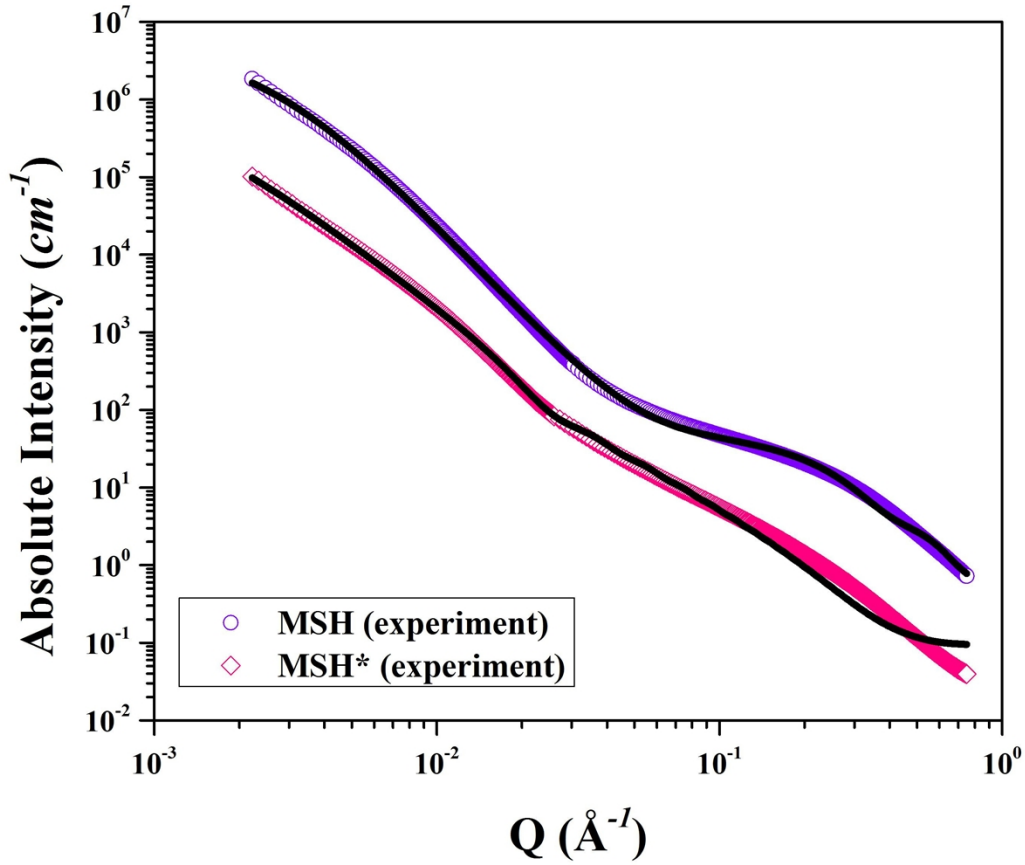


Fig. S1 The SAXS experimental data for **MSH** (violet open circle) and **MSH*** (pink open diamond). The data fitting curves using C-S-H multilayer disk-like model are denoted by black lines. The experimental and fitting intensities are shifted in y-axis by timing a factor of 10 for **MSH** for clarity. The error bars of the experimental data represent one standard deviation and are smaller than the symbols. The fitted parameters used here are listed in Table S1.

Table S1. Parameters extracted from the model fitting of SAXS data of M-S-H samples using C-S-H multilayer disk-like model^a

	D	ζ	L_2	L	\bar{n}	R	χ	Z	R_e
MSH	2.950(1)	393.13(2)	4(10)	5.0(9)	1(28)	10.42(2)	0.001(<i>lb</i>)	7(12)	6(107)
MSH*	2.487(1)	804.1(2)	0.001(<i>lb</i>)	10(66)	1(2)	162.559(8)	0.001(<i>lb</i>)	10(<i>ub</i>)	52(122)

^a*lb(ub)* means that the fitting value collapses onto the lower (upper) boundary set in the fitting procedure. The values in the parenthesis are one standard deviation from the nonlinear least-squares fitting process.

Fig. S1 shows the SAXS experimental data and the corresponding fitting curves for **MSH** and **MSH*** samples, using the C-S-H model of multilayer disk-like globules. The parameters used for data fitting are listed in Table S1. Although the experimental data and the fitting curves have acceptable agreement, the big error bars of many parameters from the fitting process shown in Table S1 indicate that C-S-H model doesn't work well for the M-S-H cases.

The IR spectra for all the gels are reported in Fig. S2 while Table S2 lists the main IR absorption peaks. The weak stretching observed near 3500 cm^{-1} in the **MSH** and **MSH*** spectra is ascribed to the characteristic Mg-OH stretch of phyllosilicates³. Moreover, absorptions near 3400 cm^{-1} and 1630 cm^{-1} are ascribed to H-bonding and hydroxyl stretching, respectively.

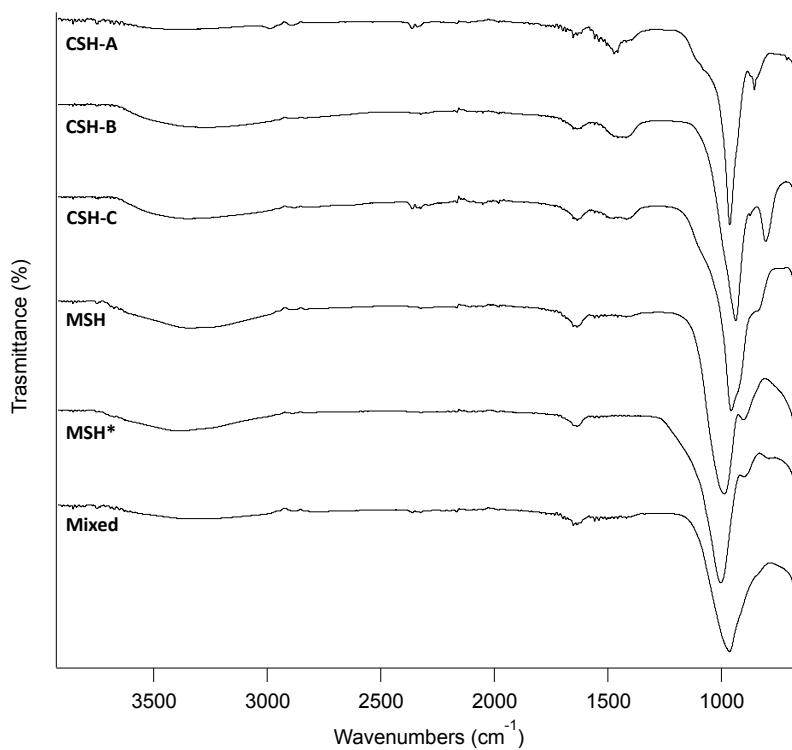


Fig. S2 ATR-FTIR spectra for **CSH-A**, **CSH-B**, **CSH-C**, **MSH**, **MSH***, and **Mixed** samples. IR absorptions near 2400 cm^{-1} are due to atmospheric CO_2 . The curves are shifted vertically for the sake of clarity.

Table S2. Infrared absorption peaks reported in the literature.³⁻⁵

Vibration/cm⁻¹		
(Mg or Ca)-O	Si-O	O-H
$\nu_s(\text{Mg-OH})$ 3500	$\nu_s(\text{Si-O})$ Q ¹ 800-910	H _{bonding} 3400
$\nu_s(\text{Ca-OH})$ 3460	$\nu_s(\text{Si-O})$ Q ² 960-1000	$\nu_s(\text{O-H})$ 1630
$\nu_s(\text{Ca-O})$ 1420-1480 (Calcite)		

The very strong band between 980 and 960 cm⁻¹ is due to Si-O stretching vibrations. The FT-IR spectrum of **CSH-A** shows the characteristic signals of C-S-H gel described in previous works⁴. We can observe a main narrow band around 960 cm⁻¹ typical of the Si-O asymmetric stretching vibrations. The signals appearing around 1400-1465 cm⁻¹, characteristic of C-O stretching vibrations, may be attributed to calcium carbonate. Spectrum of the **Mixed** sample shows the simultaneous presence of both C-S-H and M-S-H absorption bands.

The ATR-FTIR spectra were recorded with a Nexus 870-FTIR (Thermo-Nicolet) spectrometer equipped with a MCT detector cooled by liquid nitrogen. All spectra were averaged with 128 scans at 2 cm⁻¹ resolution. Data collection and analysis were carried out with OMNIC software (Thermo Fisher Scientific Inc., USA). The spectra were acquired between 4000 and 650 cm⁻¹ at room temperature.

TGA was performed both to determine the effective hydration of the so-prepared samples and to confirm a low carbonation level. Hydroxide and carbonate contributions were calculated according to the literature⁶ and subtracted out from the original weight of the sample (Brucite, $\text{Mg}(\text{OH})_2$: 267-400°C; Magnesite, MgCO_3 : 400-550°C; Portlandite, $\text{Ca}(\text{OH})_2$: 350-550°C; Calcite, CaCO_3 : 550-750°C). The obtained values are reported in Table S3.

Table S3. Amounts of hydroxide and carbonate obtained by TGA. These values are calculated with respect to the total mass of the sample at 260°C.

	Hydroxide(%w/w)	Carbonate(%w/w)
MSH	14.1	9.4
MSH*	8.8	7.9
CSH-A	7.2	4.8
CSH-B	12.6	7.0
CSH-C	7.4	3.9

The reported values confirm that the synthetic approach used for preparing the samples is able to minimize the hydroxide and carbonate formation.

Table S4 lists the target Mg/Si or Ca/Si ratio of each sample together with the experimental value obtained by EDS analysis. The agreement between the calculated and the obtained ratios is good for all the six cases.

Table S4. Target and measured ratios for the synthetic metal (Ca or Si) silicate hydrate pastes

Sample	Target ratios	Measured ($\bar{x} \pm \sigma$)
MSH	Mg/Si = 1.00	Mg/Si = 0.88 ± 0.10
CSH-A	Ca/Si = 1.00	Ca/Si = 0.97 ± 0.16
CSH-B	Ca/Si = 1.40	Ca/Si = 1.46 ± 0.09
CSH-C	Ca/Si = 1.00	Ca/Si = 1.37 ± 0.30
Mixed	Mg/Ca = 1.00	Mg/Ca = 1.38 ± 0.10
	(Mg+Ca)/Si = 1.00	(Mg+Ca)/Si = 0.91 ± 0.10

References

1. W.-S. Chiang, E. Fratini, P. Baglioni, D. Liu, and S.-H. Chen, *J. Phys. Chem. C*, 2012, **116**, 5055–5061.
2. W.-S. Chiang, E. Fratini, F. Ridi, S.-H. Lim, Y.-Q. Yeh, P. Baglioni, S.-M. Choi, U.-S. Jeng, and S.-H. Chen, *J. Colloid Interface Sci.*, 2013, **398**, 67–73.
3. H. W. Marel and H. Beutelspacher, *Atlas of infrared spectroscopy of clay minerals and their admixtures.*, 1976.

4. I. García Lodeiro, D. E. Macphee, A. Palomo, and A. Fernández-Jiménez, *Cem. Concr. Res.*, 2009, **39**, 147–153.
5. G. W. Brindley, *Am. Mineral.*, 1959, **44**, 185–188.
6. N. Khan, D. Dollimore, K. Alexander, and F. W. Wilburn, *Thermochim. Acta*, 2001, **367**, 321–333.